

# A MATHEMATICAL MODEL FOR SIMULATING THE FLOW PATTERN AND LOCAL HEAT TRANSFER COEFFICIENT IN DUCTS WITH SUDDEN ENLARGEMENT

**M.K.Bassiouny, S.A.Wilson**

The University of Menoufia, Faculty of Engineering,  
Shibin El-kom, Egypt.

**S. Soliman and Y.Rihan**

Hot Laboratories Centre, Atomic Energy Authority,  
Egypt.

## ABSTRACT

This paper deals with a numerical analysis to investigate the heat transfer and the fluid flow behaviour in a rectangular (planer) or a circular (symmetrical) channel with a sudden enlargement at inlet. A mathematical model is proposed to simulate the heat transfer process inside the heat exchangers. The model is based on the conservation equations of momentum, continuity and energy. The two equations of turbulence model 'k-ε' are also applied. The implicit scheme of finite volume method is used for solving the coupled differential equations with an iterative procedure. Thereby, the degree of flow separation is varied by changing the enlargement ratio ( $\alpha$ ). The Reynolds number ranges from 3,000 to 50,000. The results show that the local heat-transfer coefficients in the separated reattached, and redeveloped regions are several times as large as those for a fully developed flow. In general, the increase of the heat-transfer coefficient owing to flow separation is accentuated as the Reynolds number increases. The point of flow reattachment is corresponding to the peak point of the Nusselt number distribution curve. Selected comparisons with previously published experimental data for air and water are included. The comparisons show a good agreement between the present model and the experimental results of different authors.

*Keywords: Mathematical model, sudden enlargement, fluid flow, heat transfer.*

## Nomenclature

$C_1$	constant for turbulence model	Nu	Nusselt number
$C_2$	constant for turbulence model	$P_f$	P-function
$C_D$	constant for turbulence model ( $C_D = 1$ )	Pr	Prandtl number
$C_p$	specific heat at constant pressure	$Pr_t$	turbulent Prandtl number
$C_T$	integration constant expressed as P-function	p	pressure
$C_\mu$	constant in turbulent eddy viscosity equation ( $C_\mu = 0.09$ )	Q	discharge
D	inner diameter of downstream heated tube	$\dot{q}$	heat flux
d	inner diameter of upstream tube	Re	Reynolds number
E	empirical constant in the logarithmic velocity distribution law ( $E = 9.793$ )	$S_\phi$	arbitrary source term of the conservation equations
H	height of the downstream heated flat duct	T	temperature
h	convective heat transfer film coefficient	$T^+$	dimensionless temperature
i	specific enthalpy	$T'$	turbulent fluctuation component of T
k	turbulence kinetic energy	u	axial velocity
M	Mach number	$u_p$	axial velocity of the cell adjacent to the wall

$u_\tau$	shear velocity at the wall $u_\tau = \sqrt{(\tau_w/\rho)}$
$u^+$	dimensionless axial velocity
$u'$	turbulent fluctuation component of $u$
$v$	velocity component normal to the wall
$v'$	turbulent fluctuation component of $v$
$x$	axial coordinate
$Y$	height of the upstream flat duct
$y$	distance normal to the duct wall
$y_p$	distance from the wall to the cell pole
$y^+$	dimensionless normal distance from the duct wall

### Greek Symbols

$\alpha$	enlargement ratio
$\Gamma_\phi$	coefficient of effective diffusivity for variable $\phi$
$\Delta$	difference
$\varepsilon$	energy dissipation rate
$\varepsilon_i$	thermal diffusivity
$\varepsilon_m$	momentum diffusivity
$\kappa$	Von Karman constant
$\lambda$	thermal conductivity
$\mu$	dynamic viscosity
$\mu_{\text{eff}}$	effective viscosity
$\mu_t$	turbulent eddy viscosity
$\rho$	density
$\sigma_\phi$	Prandtl/Schmidt number for arbitrary variable $\phi$
$\tau$	shear stress

### Subscripts

$f$	fluid
$i$	initial
$k$	turbulence kinetic energy
$p$	pole
$t$	turbulent
$w$	wall
$\varepsilon$	energy dissipation rate
$\tau$	shear
$\phi$	arbitrary variable stands for $u, v, i, k, \varepsilon$

## INTRODUCTION

The reattachment of a turbulent shear layer is an important process in a large number of practical engineering configurations, including diffusers, airfoils and combustors. In fact, a complete list of the parameters that affect reattachment has yet to be formulated. Among two-dimensional flows, the

backward-facing single step is the simplest reattaching flow. The separation line is straight and fixed at the edge of the step and there is only one separated zone instead of two, as seen in the flow over a fence or obstacle. The flow structure in case of the separated flow over a backward-facing step depends mainly on six parameters namely; the initial boundary-layer state before separation (laminar or turbulent), the initial boundary-layer thickness, the freestream turbulence, the pressure gradient, the aspect ratio and the surface roughness geometries. The first five parameters are discussed in details by Eaton and Johnston [1] and the last parameter is investigated experimentally by Kim and Chung [2].

In many engineering applications, specially in the field of heat exchangers, the fitting of tubes inside or outside the heat exchanger yields a sudden enlargement or contraction zone. In this zone, the recirculation motion or the back flow of the fluid affects directly the pressure recovery, the local heat transfer and the velocity profile along the flow duct. One of the important factors influencing the local heat transfer coefficient is the enlargement ratio  $\alpha$ . The other factors are the operating conditions like the initial fluid velocity, wall temperature, turbulence level and others. This type of flow is termed as flow behind double backward facing steps. Abbott et. al. [3] correlate an empirical formula from their experimental data to define the local coefficient of heat transfer in flat ducts. Their results on turbulent incompressible fluid flow indicate that, stalls of different lengths are produced on the two duct walls downstream of the double step. The experimental data demonstrated that once the stall positions are established, the short and long stalls remain stable in either positions but may be readily interchanged by temporarily inserting a vane in the flow. Other investigators [4] studied the hydrodynamic characteristics of the turbulent flow through abrupt tube. Boelter, et. al [5] studied the phenomena for a compressible fluid inside a circular cross-section pipe under a constant wall temperature, while Krall & Sparrow [6] employed water as a working fluid. Their investigations were performed under constant wall heat flux. Filetti & Kays [7] presented empirical formulae for calculating the maximum Nusselt number of air flow through a flat duct for both short and long stall conditions.

Since in literatures, there are still insufficient information about the effect of the sudden enlargement at the inlet ports of a heat exchanger on the flow field and the heat transfer characteristics as well as on its performance, the purpose of the present paper is to establish a mathematical model to simulate the flow inside heat exchangers (either tube or flat ducts) with sudden enlargement at the inlet ports. Thereby, the governing differential equations are solved together using an implicit scheme of finite volume method with an iterative procedure [8]. In the following, the details of the numerical treatment are presented.

MATHEMATICAL MODEL

In the analysis, an incompressible fluid ( $M < 0.1$ ) is assumed to enter a tube or a flat duct with a sudden enlargement. The wall temperature of the duct is taken to be constant. The physical domain of the present work is shown in Figure (1), while Figure (2) represents the grid system used for the numerical treatments. The use of the dense grids adjacent to the step wall is essential to ensure adequate number of grid inside the separation zone. This leads to reasonable descritization process inside the very high pressure gradient zone. The details of the proposed mathematical model and the solution technique are given as follows:

Governing Equations

The fluid flow is considered as turbulent, incompressible and two-dimensional in space. The strongly coupled set of partial differential equations representing the conservation of mass, momentum and energy are employed. In addition of this, the modified form of turbulence model 'k-ε' is used also during the solution procedure. The general form of the conservation equations can be written in the following form:

$$\frac{\partial}{\partial x} [\rho u \phi - \Gamma_\phi \frac{\partial u}{\partial x}] + \frac{\partial}{\partial y} [\rho v \phi - \Gamma_\phi \frac{\partial u}{\partial y}] = S_\phi \quad (1)$$

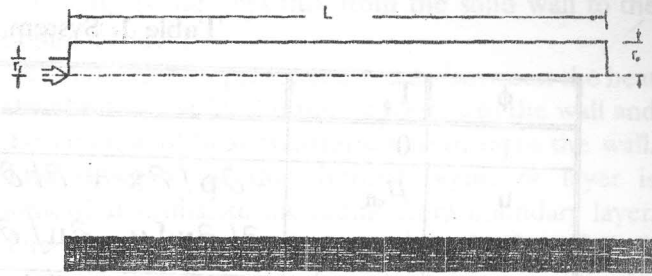


Figure 1. Physical domain and the construction of grid used in the present work.

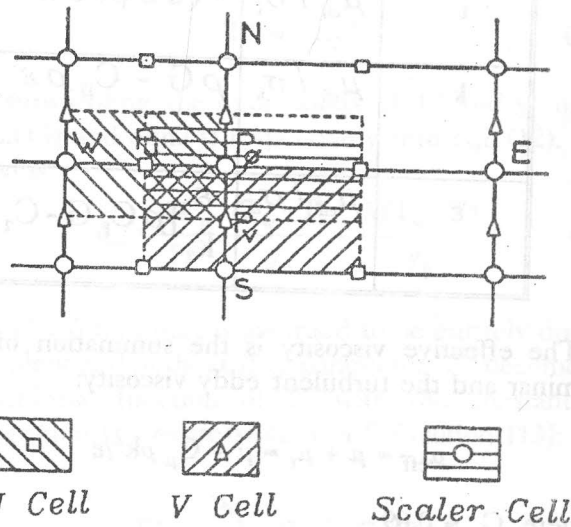


Figure 2. The grid used in the numerical solution.

where  $\phi$  stands for the arbitrary variables of the flow field,  $\Gamma_\phi$  is the coefficient of effective diffusivity and  $S_\phi$  is the source term of the conservation equation. The value of  $\phi$ ,  $\Gamma_\phi$  and  $S_\phi$  are given in Table (1) where the turbulence constants used in the turbulence model has the following values [9]:

$$\sigma_i = 1, \sigma_k = 1, \sigma_\epsilon = 1.3, C_D = 1, C_1 = 1.44, C_2 = 1.92,$$

and

$$G = C_\mu \frac{k}{\epsilon} \{ 2 [ (\frac{\partial u}{\partial x})^2 + (\frac{\partial v}{\partial y})^2 ] + [ \frac{\partial u}{\partial y} + \frac{\partial v}{\partial x} ]^2 \} \quad (2)$$

Table 1. System of differential equations.

$\phi$	$\Gamma_\phi$	$S_\phi$	remarks
1	0	0	continuity
u	$\mu_{\text{eff}}$	$-\partial p / \partial x + \partial / \partial y (\mu_{\text{eff}} \partial v / \partial x) + \partial / \partial x [\mu_{\text{eff}} \partial u / \partial x - 2/3 (\mu_{\text{eff}} \nabla u + \rho k)]$	axial momentum
v	$\mu_{\text{eff}}$	$-\partial p / \partial y + \partial / \partial y [(\mu_{\text{eff}} \partial v / \partial y) - 2/3 (\mu_{\text{eff}} \nabla u + \rho k)]$	momentum in y-direction
i	$\mu_{\text{eff}} / \sigma_i$	$-(u \partial p / \partial x + v \partial p / \partial y)$	energy
k	$\mu_{\text{eff}} / \sigma_k$	$\rho G - C_D \rho \varepsilon$	turbulence kinetic energy
$\varepsilon$	$\mu_{\text{eff}} / \sigma_\varepsilon$	$\frac{\varepsilon}{k} [\rho C_1 G - C_2 \rho \varepsilon]$	energy dissipation rate

The effective viscosity is the summation of the laminar and the turbulent eddy viscosity:

$$\mu_{\text{eff}} = \mu + \mu_t = \mu + C_\mu \rho k^2 / \varepsilon \quad (3)$$

where,  $C_\mu = 0.09$

**Boundary Conditions**

A special treatment of the flow adjacent to the wall is considered. The wall function [10] is used for modifying the flow parameters inside the boundary layer. The fluid flow near the wall is considered as one dimensional and constant shear stress as well as constant heat flux layer for each cell and can be varied from one cell to another. The depth of different boundary layer zones were obtained from the experimental data of Hinze [11] as follows:

- $y^+ < 5$  the flow is in the viscous sublayer,
- $5 < y^+ < 30$  the flow is in the buffer zone,
- $y^+ > 30$  the flow is in the free turbulent zone.

where

$$y^+ = \rho u_\tau y_p / \mu \quad (4)$$

is the dimensionless distance from the duct wall. The flow parameter near the wall is modified according to the following scheme:

**1- Velocities "u or v" :**

If the grid points adjacent to the wall lie inside the viscous sublayer then

$$\tau = -\mu \frac{\partial u}{\partial y} = -\mu \frac{u_p}{y_p} \quad (5)$$

If the points lie outside the viscous sublayer ( $y^+ > 5$ ) then the logarithmic velocity distribution is used [10]

$$u_p / u_\tau = \frac{1}{\kappa} \ln E y^+ \quad (6)$$

where,

$E = 9.793$ , stands for the effect of wall friction due to roughness [12],

$\kappa = 0.4187$ , Von Karman's constant [11].

The wall shear stress is given by



$$\tau = \left[ \frac{\rho C_\mu^{1/4} k^{1/2}}{\kappa \ln E y^+} \right] u_p \quad (7)$$

### 2. Turbulence Kinetic Energy "k" :

In case of turbulent kinetic energy, the source term involving the generation of turbulence near the wall is modified by replacing the term  $\mu_{eff} \left( \frac{\partial u}{\partial y} \right)^2$  with  $\left( \tau_w \frac{u_p}{y_p} \right)$  which is the generation term for the Couette flow. Linearizing the source term, the following form is obtained [12]:

$$S_k = S_{u_k} + S_{p_k} k \quad (8)$$

where,

$$S_{p_k} = \rho C_\mu^{3/4} k^{1/2} \frac{y^+}{y_p} \quad (9)$$

for  $y^+ < 5$ , and

$$S_{p_k} = \rho C_\mu^{3/4} k^{1/2} \left( \frac{\ln E y^+}{\kappa y_p} \right) \quad (10)$$

for  $5 < y^+ < 30$ .

### 3. Energy Dissipation Rate "ε" :

The value of energy dissipation rate can be calculated from the following equation, see Ref. [12],

$$\epsilon = \frac{C_\mu^{3/4} k^{3/2}}{\kappa y_p} \quad (11)$$

### 4. Temperature :

This model is derived for constant heat flux on each cell across the thermal boundary layer. The following form of the nondimensional temperature  $T^+$  is considered [13]:

$$T^+ = \frac{\rho C_p u_\tau (T_w - T)}{\dot{q}_w} \quad (12)$$

where  $\dot{q}_w$  is the heat flux from the solid wall to the boundary layer.

This quantity represents the ratio between the heat absorbed or lost by the fluid adjacent to the wall and the amount of heat transferred from or to the wall. The structure of the thermal boundary layer is somewhat similar to the momentum boundary layer. The distinguishing value of  $y^+$  is 5. For  $y^+ < 5$ , transport is assumed to be solely due to molecular activity and the expression for the heat flux parameter  $T^+$  may be calculated from the following equation:

$$T^+ = Pr_t y^+ \quad (13)$$

By substituting the expressions of  $T^+$  and  $y^+$  using eqn.(13) and eqn.(4) respectively into eqn.(12), one obtains

$$\dot{q}_w = \frac{\mu C_p}{Pr_t} \frac{(T_w - T)}{y_p} = \frac{\lambda (T_w - T)}{y_p} \quad (14)$$

For  $y^+ > 5$  transport is assumed to be entirely due to turbulence. The heat flux parameter  $T^+$  becomes a logarithmic function of  $Y^+$  with the constant of integration  $C_T$  expressible as a P-function [13]:

$$\begin{aligned} T^+ &= \frac{Pr_t}{\kappa} \ln E y^+ + C_T(Pr) \\ &= Pr_t \left[ u^+ + P_f \left( \frac{Pr}{Pr_t} \right) \right] \end{aligned} \quad (15)$$

Therefore, the wall heat flux may be calculated from the following relation:

$$\dot{q}_w = \frac{\rho C_p C_\mu^{1/4} k^{1/2} (T_w - T)}{Pr_t \left[ u^+ + P_f \left( \frac{Pr}{Pr_t} \right) \right]} \quad (16)$$

In the literature, many forms of the P-function are available. One of them is that of Spalding and Jayatillaka [14], which is valid for impermeable smooth walls

$$P_f = 9.24 \left[ \left( \frac{Pr}{Pr_t} \right)^{0.75} - 1 \right] \left[ 1 + 0.28 e^{-0.007 \left( \frac{Pr}{Pr_t} \right)} \right] \quad (17)$$

Another relations of different authors [15,16], may

be recasted in the following forms:

$$P_f = 9.24 \left[ \left( \frac{Pr}{Pr_t} \right)^{0.75} + 1 \right] \quad (18)$$

and,

$$P_f = 9 \left[ \left( \frac{Pr}{Pr_t} \right) - 1 \right] \left( \frac{Pr}{Pr_t} \right)^{-0.25} \quad (19)$$

Thereby, the turbulent Prandtl number ( $Pr_t$ ) is defined as

$$Pr_t = \epsilon_m / \epsilon_1 = [\overline{u'v'} / (\partial u / \partial y)] / [\overline{T'v'} / (\partial T / \partial y)] \quad (20)$$

which is the ratio between the turbulent momentum diffusivity and the turbulent thermal diffusivity. The value of  $Pr_t$  may be taken between 0.85 and 1. Especially for air as a working fluid, Kays and Muffat [17] suggested a correlation for  $Pr_t$  as a function of  $y^+$  as follows:

$$Pr_t = 0.9 + 0.35 [ 1 + \cos (\pi y^+ / 37) ] \quad (21)$$

The foregoing correlation is valid only for  $y^+ < 37$ . If  $y^+$  takes values greater than 37,  $Pr_t$  will become constant and equals to 0.9.

Figure (3) represents a comparison between the local Nusselt number distribution at different P-functions. In the present work, it is found that the  $P_f$  given by eqn.(17) gives the best prediction compared with the experimental data.

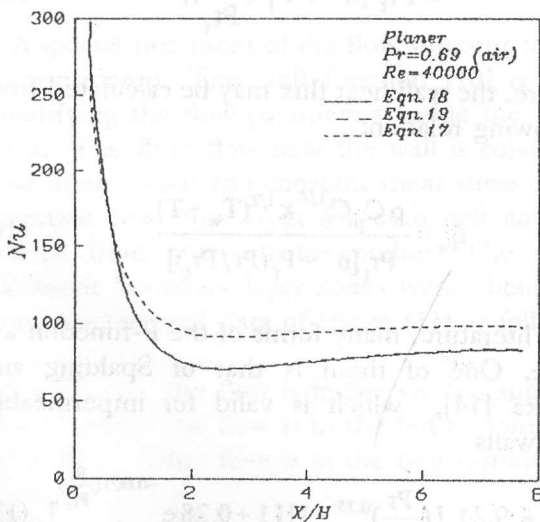


Figure 3. Effect of P-function.

## RESULTS AND DISCUSSION

Figure (4) shows a comparison between the present model and the experimental results of Filetti and Kays [7] for the variation of the local Nusselt number as a function of normalized distance near the entrance to a flat duct (planer) with  $\alpha = 2.12$  in which there is an abrupt symmetrical enlargement in flow cross-section. Heat transfer data were compared for both short stall (Figure 4a) and long stall (Figure 4b). The two figures pertain to flow at a Prandtl number of 0.69. On each of these plots, Reynolds number is the parameter having values of 69800, 103500 and 130000. It is clear from the figures that there is a fair agreement between the present numerical results and the experimental data [7]. It is found also that, for a given condition (i.e. a given Re, Pr and  $\alpha$ ), the local Nusselt number exhibits a clearly defined maximum at a position that lies somewhere between 0.5 and 0.75 the duct height from the onset of separation. The location of the maximum is believed to coincide with the point of flow reattachment. This interpretation is consistent with interpretations of experimental results of Abbott and Kline[3] as well as Filetti and Kays [7]. Downstream of the point of reattachment, Nusselt number decays, apparently toward the value for fully developed duct flow. The separated region lies upstream of the point of reattachment and the redevelopment region lies downstream of this point.

Figure (5) presents a comparison between the present model and the experimental results [13] for a flow of air ( $Pr=0.69$ ) through a tube without sudden enlargement ( $\alpha=1$ ) at a Reynolds number of 17000. It can be clearly seen that the difference between both experimental and theoretical results is acceptable.

Another comparison between the numerical model considered and the experimental data of Kral and Sparrow [6] for the effect of flow separation on the heat transfer characteristics of a turbulent pipe flow with  $\alpha=2$  is represented in Figure (6a) in case of  $Pr=3$  and in Figure (6b) in case of  $Pr=6$ . The two figures indicate a good agreement between both results.

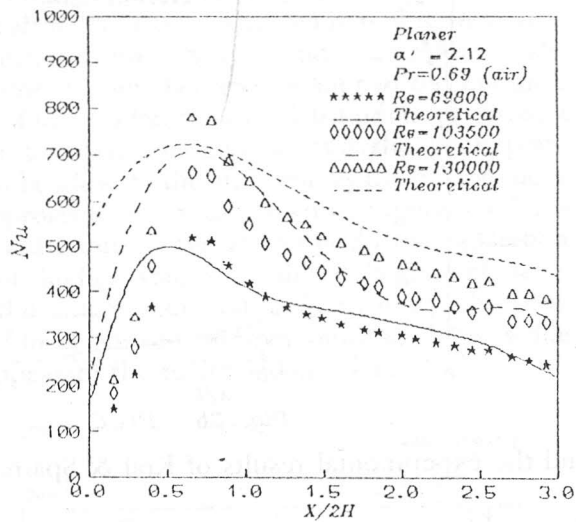


Fig. 4a : Short stall.

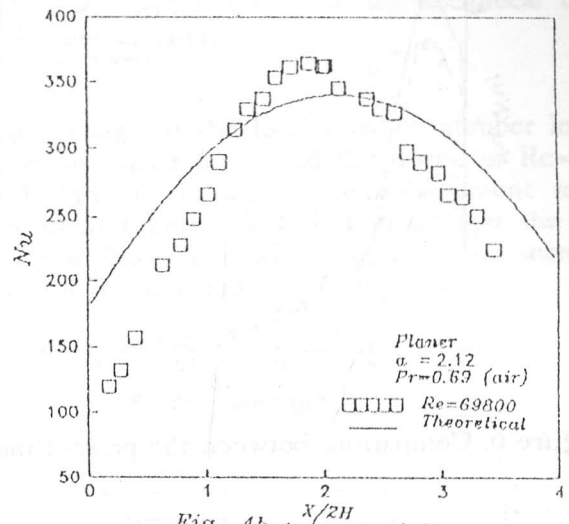


Fig. 4b : Long stall.

Figure 4. Comparison between the present model and the experimental results Filetti & Kays [7].

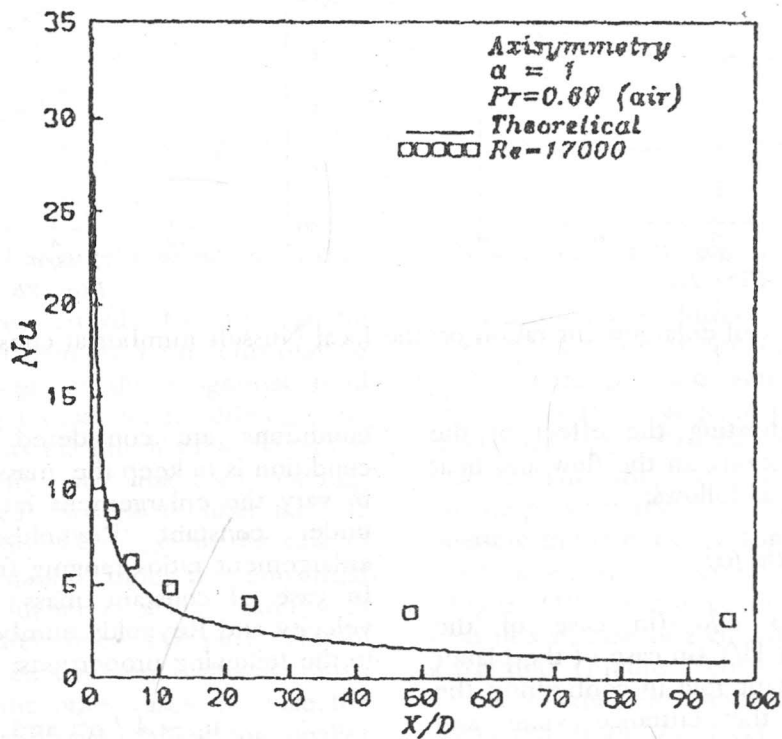


Figure 5. Comparison between the present model and the experimental results of Bird [13].

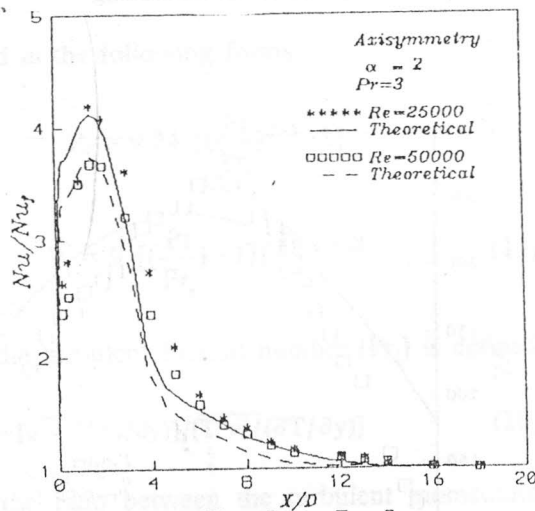


Fig. 6a : Pr=3.

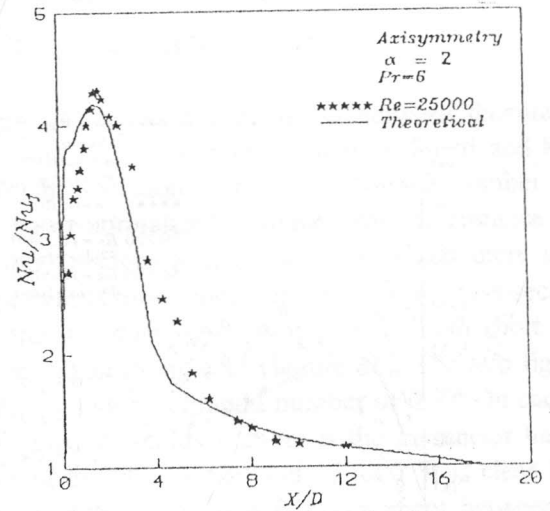


Fig. 6b : Pr=6.

Figure 6. Comparison between the present model and the experimental results of Kral & Sparrow [6]

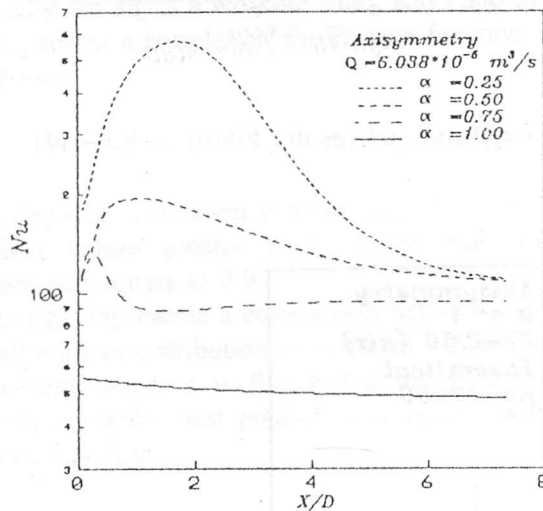


Fig. 7a

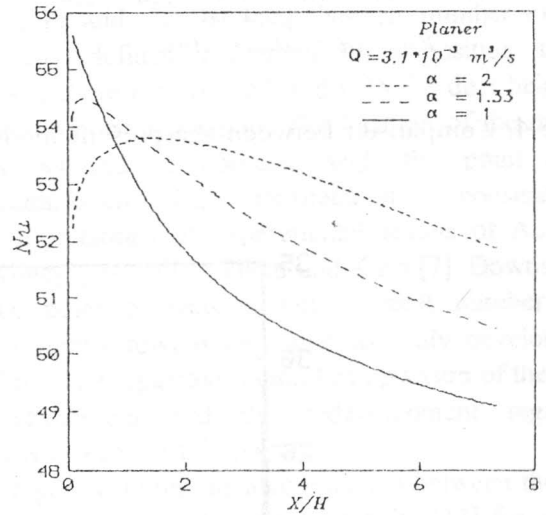


Fig. 7b

Figure 7. Effect of enlargement ratio on the local Nusselt number at constant flow rate.

A parametric study indicating the effect of the different operating conditions on the flow and heat transfer process is made as follows:

*Effect of Enlargement Ratio ( $\alpha$ )*

The enlargement ratio  $D/d$  (in case of the axisymmetric domain) or  $H/Y$  (in case of the planer domain) plays an important role in configuring the geometrical shape of the entrance zone and consequently the structure of the flow behind the step. This zone is defined as the recirculation zone. In order to clear this effect, two different operating

conditions are considered. The first operating condition is to keep the mass flow rate constant and to vary the enlargement ratio. The second run is under constant Reynolds number. Thereby enlargement ratios ranging from 1 to 4 are applied. In case of constant mass flow rates, the initial velocity and Reynolds number are varied according to the following proportions:

$$u_i \sim 1 / \alpha^2, \text{ and } Re_i \sim 1/\alpha$$



When the enlargement ratio increases, the corresponding initial velocity decreases with the reciprocal of its square. This leads to a reduction in the recirculation zone and therefore, the reattachment point becomes nearer to the entrance region. The resultant local distribution of Nusselt number decreases in general and the peak point tends to be close to the step wall as the enlargement ratio approaches unity as shown in Figure (7). This can be attributed to the reduction in the separation zone for higher values of the enlargement ratio. When the enlargement ratio equals unity, the peak value of local Nusselt number vanishes. This is due to disappear of the recirculation zone.

The second operating condition is the case of constant Reynolds number. The initial velocity in this case is proportional to the reciprocal of the enlargement ratio

$$u_i \sim 1 / \alpha$$

The change in the local Nusselt number in both cases of axisymmetry and flat ducts for  $Re=30000$  and different values of the enlargement ratio is shown in Figure (8). It is noticed that the initial value of Nusselt number increases with increasing the enlargement ratio.

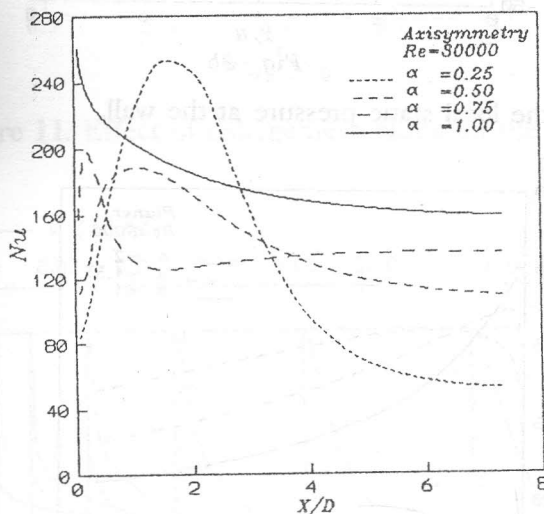


Fig. 8a

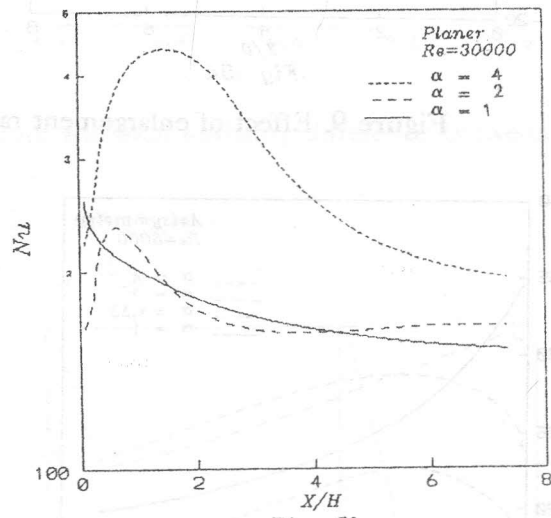


Fig. 8b

Figure 8. Effect of enlargement ration on the local Nusselt number at constant Reynolds number.

The peak point moves towards the step wall for higher values of the enlargement ratio. This may be attributed to the change in the tangential fluid velocity inside the separation zone. Although the initial velocity reaches its minimum value when the enlargement ratio equals unity, the corresponding distribution for the local Nusselt number has the greatest magnitude. This is because in the case of absence of the recirculation zone, the tangential velocity to the wall has higher values compared with those having recirculation zones. The peak value in case of the smallest enlargement ratio is much greater than those of the other cases, because the initial jet velocity has higher values for smaller enlargement ratios. This makes the reattachment point to take a long distance from the step wall. In addition of this, the high value of the initial velocity reflects in turn on the tangential velocity at this

point in such a condition which leads to an increase in the peak value of Nusselt number.

The static pressure along the wall is affected directly by the change in the enlargement ratio as shown in Figure (9). Decreasing the value of the enlargement ratio, the diffuser effect will increase. So, the pressure recovery will increase. The negative pressure in the entrance zone returns to the effect of the flow separation behind the step wall.

Figure (10) represents the local distribution of the heat flux in case of a circular duct (Figure 10a) and a flat duct (Figure 10b) for  $Re=6000$  and different values of the enlargement ratio. This figure is calculated from the local distribution of Nusselt number and the temperature distribution of the fluid near the wall

$$q = h \cdot \Delta T = f(Nu, T_p).$$

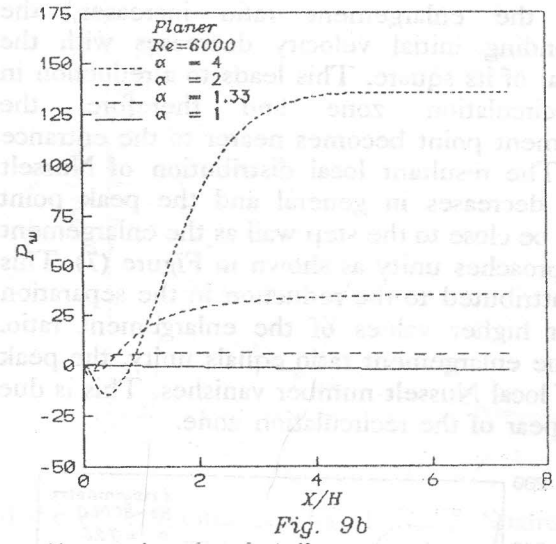
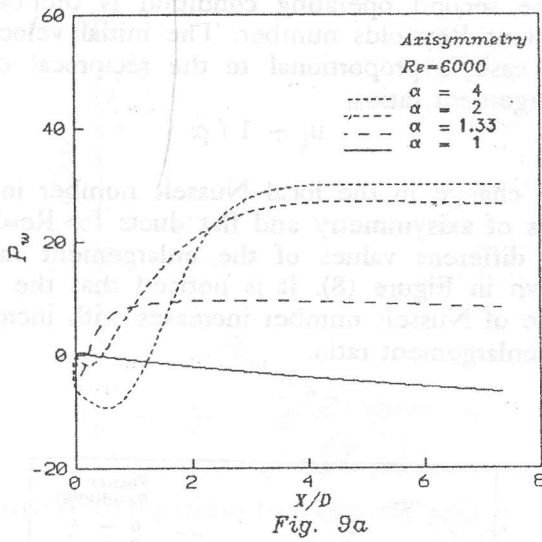


Figure 9. Effect of enlargement ration on the local static pressure at the wall.

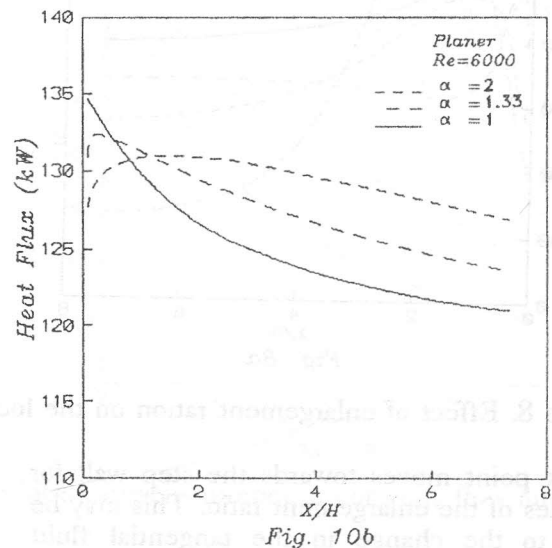
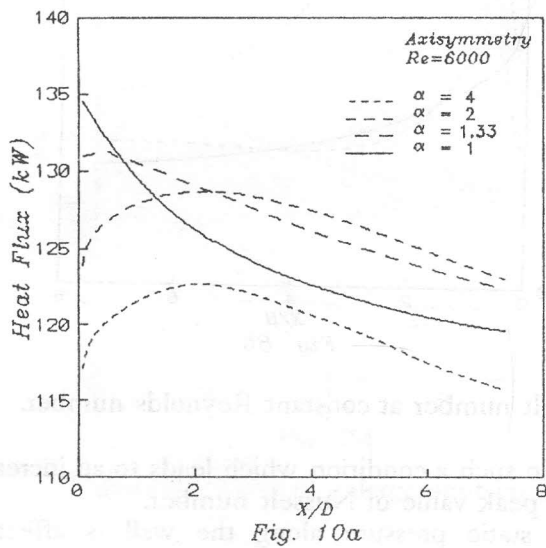


Figure 10. Effect of enlargement ration on the heat flux distribution

This can interpret the increase in the heat flux with increasing the enlargement ratio. The same conclusion is obtained in Figure (11), which represents the variation of the mean temperature or total enthalpy difference between inlet and outlet of the duct with the enlargement ratio at  $Re=30000$ , also for the above mentioned two cases of axisymmetry (Figure 11a) and flat ducts (Figure 11b). The trend of the curves can be attributed to the decrease in the mean velocity at exit with decreasing the enlargement ratio. This leads to an increase in the residence time of the fluid inside the

duct and consequently an increase in the fluid temperature and enthalpy. The turbulence kinetic energy and its dissipation rate in both cross-sections along the flow channels are obtained and indicated in Figure (12) for a constant value of  $Re$  and different values of  $\alpha$ . The figure illustrates the effect of the wall on vanishing the turbulence kinetic energy and dissipation rate and also the effect of the enlargement ratio  $\alpha$  on both  $k$  and  $e$  profiles especially inside the recirculation zone at which the turbulence kinetic energy takes its peak value.

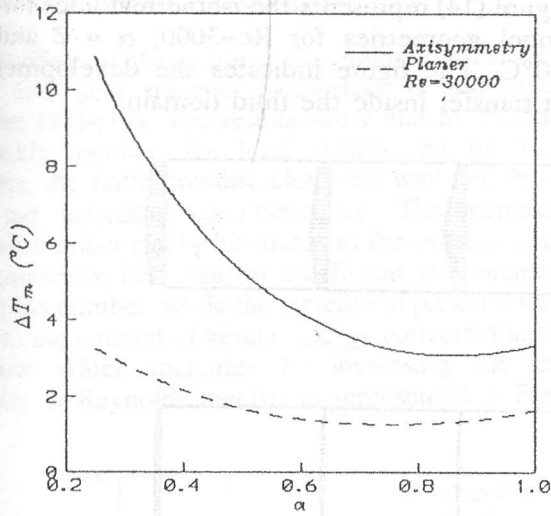


Fig. 11a

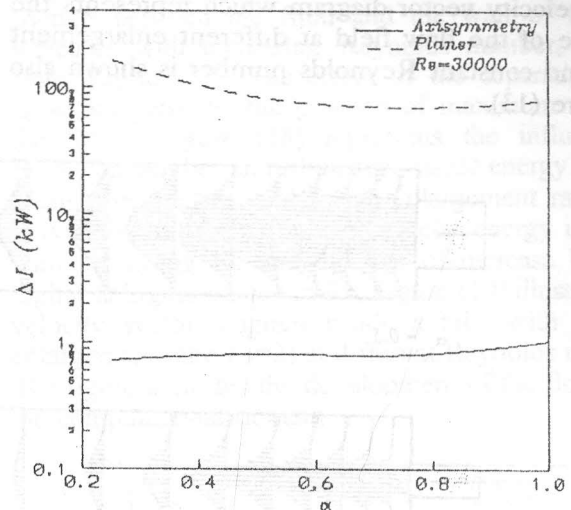


Fig. 11b

Figure 11. Effect of enlargement ration on the temperature and total enthalpy difference between inlet and exit.

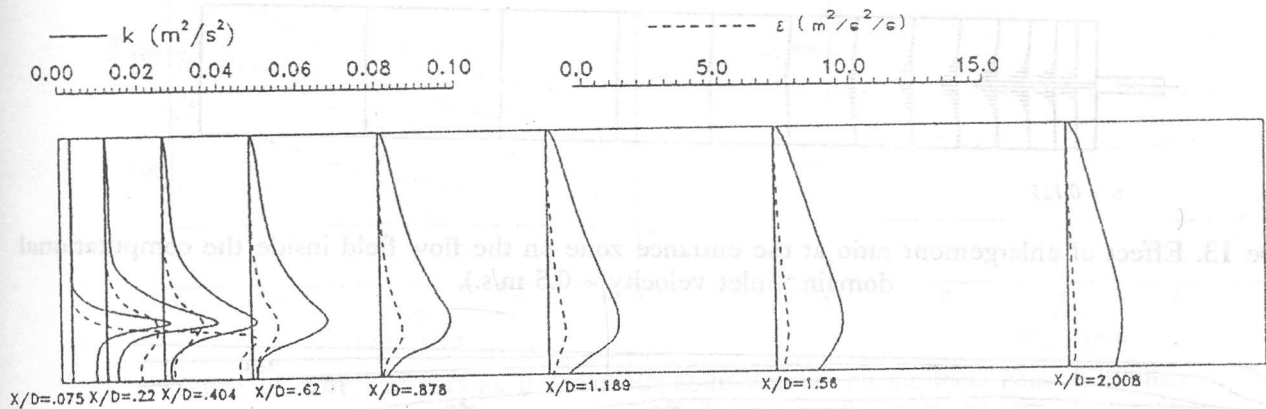


Fig.12a : Axisymmetric,  $\alpha = 4$ ,  $Re=6000$ .

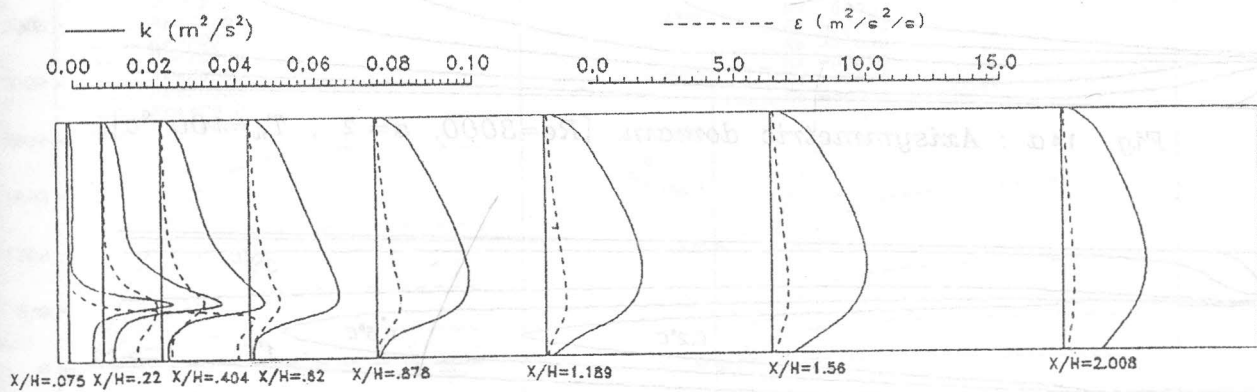


Fig.12b : Planer,  $\alpha = 4$ ,  $Re=6000$ .

Figure 12. Turbulence kintic energy & dissipation rate at different cross-sections.

The velocity vector diagram which represents the structure of the flow field at different enlargement ratios and constant Reynolds number is shown also in Figure (13).

Figure (14) represents the isothermal lines for both channel geometries for  $Re=3000$ ,  $\alpha = 2$  and  $T_w=100^\circ\text{C}$ . The figure indicates the development in heat transfer inside the fluid domain.

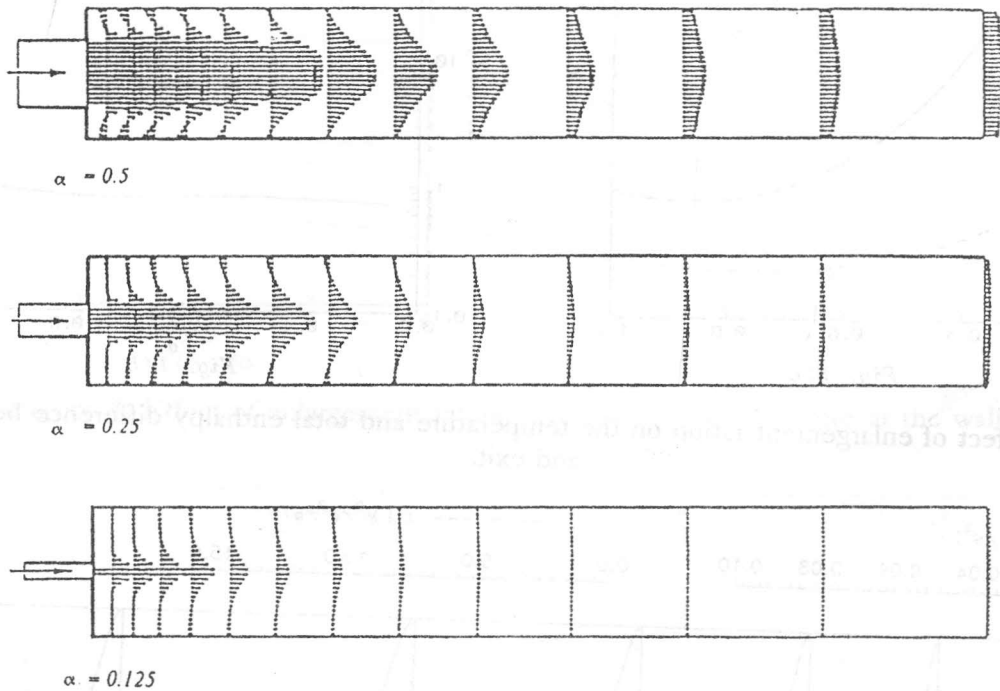


Figure 13. Effect of enlargement ratio at the entrance zone on the flow field inside the computational domain. (inlet velocity = 0.5 m/s.).

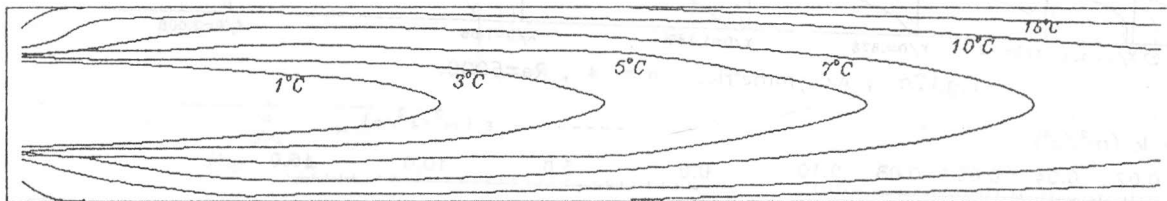


Fig. 14a : Axisymmetric domain. [ $Re=3000$ ,  $\alpha=2$ ,  $T_w=100^\circ\text{C}$ ]

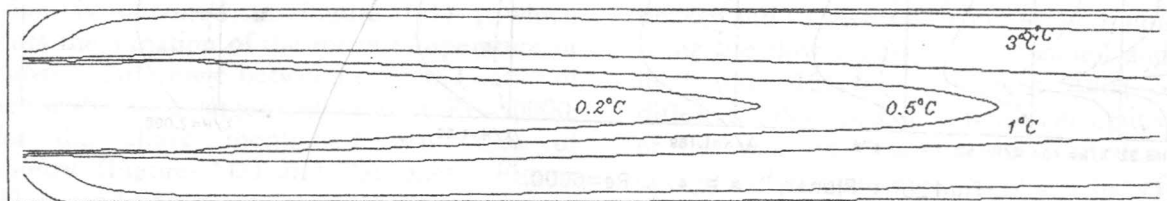


Fig. 14b : Planer domain. [ $Re=3000$ ,  $\alpha=2$ ,  $T_w=100^\circ\text{C}$ ]

Figure 14. Isothermal lines.



*Effect of Reynolds Number (Re)*

The effect of the entrance Reynolds number on the flow and heat transfer parameters is indicated in Figures (15)-(19). The results show that by increasing Reynolds number, the local distribution of Nusselt number, the static pressure along the wall and the heat flux are increased simultaneously. The increase in Nusselt number can be attributed to the enhancement of the convective heat transfer coefficient with increasing Reynolds number, while the increase in pressure returns back to the amount of kinetic energy converted to static pressure which increases by increasing the initial velocity or Reynolds number as represented in Figure

(16). The coefficient of shear stress, resulting from the friction between the fluid and the wall of the duct increases with increasing Reynolds number, as seen from Figure (17). The effect of the separation zone appears clearly on the position of maximum value of the S.S.C. Figure (18) represents the influence of Reynolds number on turbulence kinetic energy for both channel geometries and for an enlargement ratio  $\alpha=2$ . It is clear that the turbulence kinetic energy increases with increasing Re and the rate of increase becomes higher at higher values of Re. Figure (19) illustrates the velocity vector diagram inside a tube with constant enlargement ratio ( $\alpha=2$ ) at different Reynolds numbers. The figure indicates the development of the flow along the computational domain.

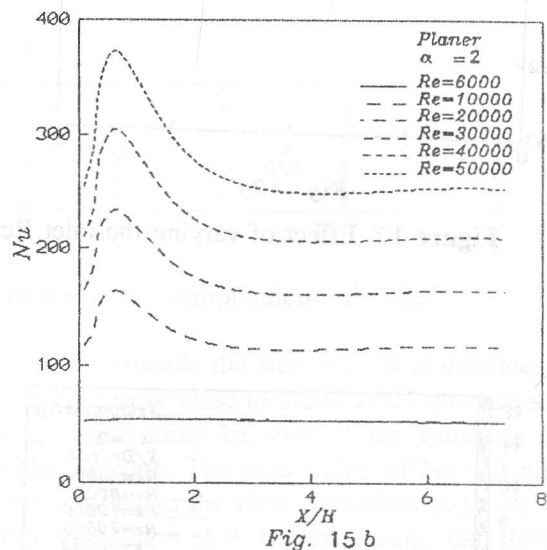
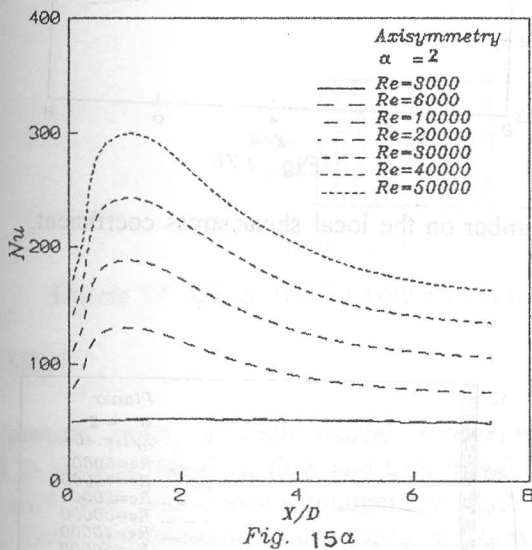


Figure 15. Effect of varying the inlet Reynolds number on the local Nusselt number.

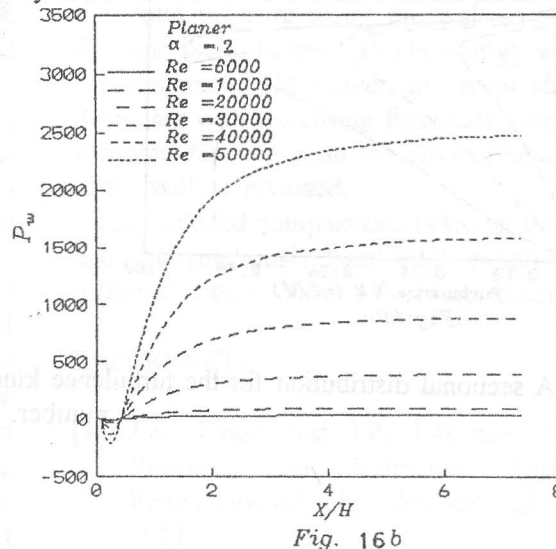
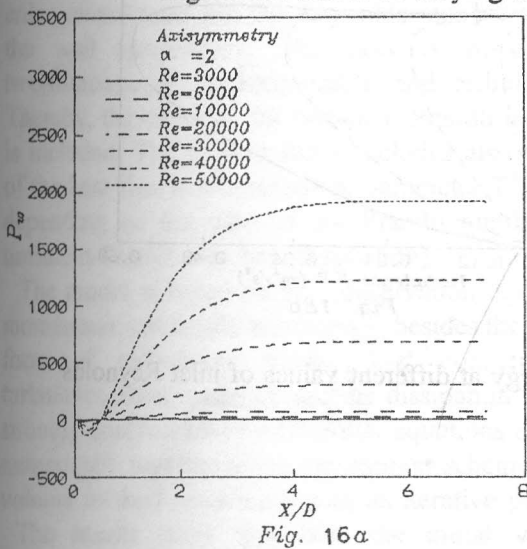


Figure 16. Effect of varying the inlet Reynolds number on the static pressure distribution along the wall.

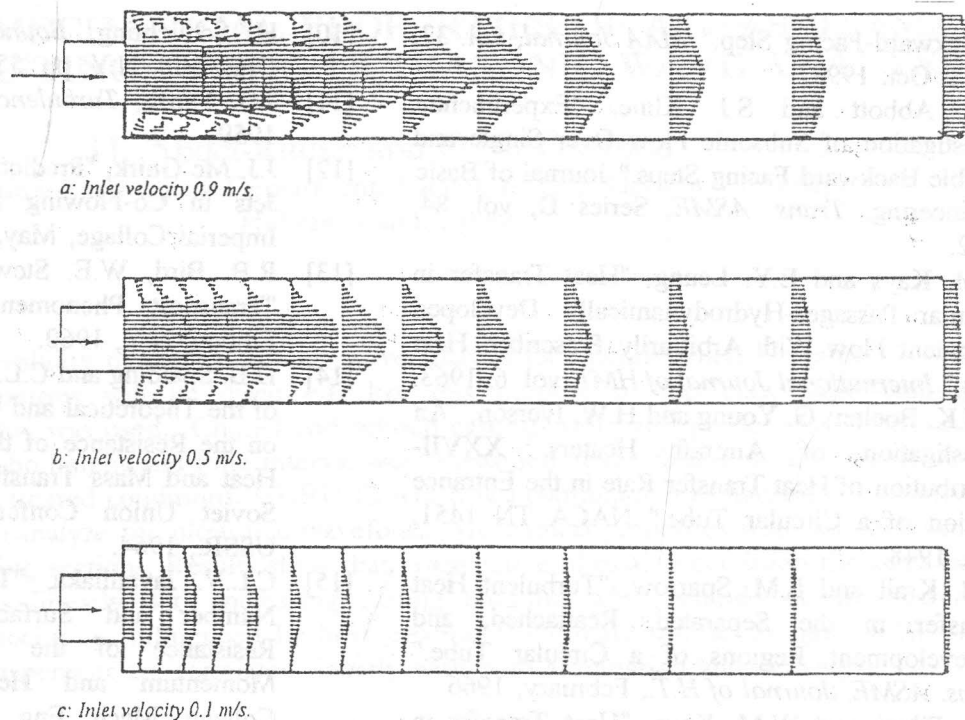


Figure 19. Effect of inlet velocity on the flow field inside the computational domain.

## CONCLUSION

In the present paper, a mathematical model is introduced to simulate the fluid flow and heat transfer in a heat exchanger with sudden enlargement at the inlet port. Both axisymmetric and rectangular flow channels are taken into account under varying the enlargement ratio and the Reynolds number as well as the wall temperature. The flow is considered as two-dimensional, incompressible and turbulent flow. Thereby, the effect of the turbulent Prandtl number  $Pr_t$  is included. The present study includes also the effect of the heat flux nondimensional parameter  $T^+$ , which is depending on the ratio of the Prandtl number to the turbulent Prandtl number (P-function).

The model is based on the conservation equations of momentum, continuity and energy, besides the modified form of turbulence model 'k- $\epsilon$ ' concerning the turbulence kinetic energy and its dissipation rate. The strongly coupled set of differential equations are solved numerically together using the implicit scheme of finite volume method combining with an iterative procedure.

The results show that both the initial values of Nusselt number and the heat flux at the wall increase with increasing the enlargement ratio ( $\alpha$ ) and the peak

point moves towards the step wall as  $\alpha$  increases until it becomes exactly close to the channel entrance section when  $\alpha$  equals unity because of the vanishing of the recirculation zone. The peak value of Nusselt number is corresponding to the flow reattachment point. It can be also concluded that by increasing the Reynolds number, the local distribution of Nusselt number and the static pressure along the wall as well as the heat flux and the turbulence kinetic energy will be increased simultaneously. Moreover, the shear stress coefficient decreases with increasing Reynolds number to a certain location depending on the enlargement ratio, then its effect will be reversed.

The included comparisons between the present model and the previously published experimental data of different authors show a fairly agreement.

## REFERENCES

- [1] J.K. Eaton and J.P. Johnston, "A Review of Research on Subsonic Turbulent Flow Reattachment." *AIAA Journal*, vol. 19, No. 9, Sep. 1981.
- [2] B.N. Kim and M.K. Chung, "Experimental Study of Roughness Effect on the Separated Flow Over

- a Backward-Facing Step." *AIAA Journal*, vol. 33, No. 1, Oct. 1994.
- [3] D.E. Abbott and S.J. Kline, "Experimental Investigation of Subsonic Flow Over Single and Double Backward Facing Steps." *Journal of Basic Engineering, Trans. ASME, Series D*, vol. 84, 1962.
- [4] W.M. Kays and E.Y. Leung, "Heat Transfer in Annular Passages-Hydrodynamically Developed Turbulent Flow With Arbitrarily Prescribed Heat Flux." *International Journal of HMT*, vol. 6, 1963.
- [5] L.M.K. Boelter, G. Young and H.W. Iverson, "An Investigation of Aircraft Heaters, XXVII-Distribution of Heat Transfer Rate in the Entrance Section of a Circular Tube." NACA TN 1451, July, 1948.
- [6] K.M. Krall and E.M. Sparrow, "Turbulent Heat Transfer in the Separated, Reattached, and Redevelopment Regions of a Circular Tube." *Trans. ASME, Journal of H.T.*, February, 1966.
- [7] E.G. Filetti and W.M. Kays, "Heat Transfer in Separated, Reattached, and Redevelopment Regions Behind a Double Step at Entrance to a Flat Duct." *Trans. ASME, Journal of H.T.*, May 1967.
- [8] S.V. Patankar, "Numerical Heat Transfer and Fluid Flow." Hemisphere Publishing Corporation, 1980.
- [9] B.E. Launder and D.B. Spalding, "Mathematical Models of Turbulence." Academic Press, London & NY, 1972.
- [10] H. Schlichting, *Boundary Layer Theory*, Mc Graw Hill, N.Y, pp. 553-586, 1968.
- [11] J.O. Hinze, *Turbulence*, Mc Graw Hill, N.Y, 1959.
- [12] J.J. Mc Guirk, "Prediction of Turbulent Bouyant Jets in Co-Flowing Streams." *Ph.D. Thesis*, Imperial Collage, May, 1975.
- [13] R.B. Bird, W.E. Stewart and E.N. Lightfoot, "Transport Phenomena." Wiley International Edition, N.Y, 1960.
- [14] D.B. Spalding and C.L.V. Jayatillaka, "A Survey of the Theoretical and Experimental Information on the Resistance of the Laminar Sub-Layer to Heat and Mass Transfer." Proceedings 2nd All Soviet Union Conference on HMT Minsk, USSR., 1964.
- [15] C.L.V. Jayatillaka, "The Influence of Prandtl Number and Surface Roughness on the Resistance of the Laminar Sub-Layer to Momentum and Heat Transfer." Imperial College, Mech. Eng. Dep., Report TWF/R/2, 1966.
- [16] B.E. Launder and D.B. Spalding, "The Numerical Computation of Turbulent Flows." Imperial College, M.E.D., Report HTS/73/2, 1973.
- [17] W.M. Kays and R.J. Muffat, "The Behaviour of Transpired Turbulent Boundary Layers." Academic press, Edition by Launder, B.E., 1975.
- [18] Launder "Studies in Convection." *Academic Press*, 1975.